(Preprint) AAS 22-707

FEASIBILITY STUDIES FOR AN AUTONOMOUS CISLUNAR POSITION, NAVIGATION AND TIMING CONSTELLATION

Dhathri H. Somavarapu*, Davide Guzzetti†, Siamak Hesar‡

In this paper, we present the feasibility studies' results for an autonomous persistent cislunar position, navigation, and timing (PNT) constellation. We conducted analyses on orbit and constellation design, established baseline metrics for PNT service provision and assessed the feasibility based on coverage metrics. As a result of these studies, we set potential baseline orbit and constellation configurations that achieve target metrics for coverage for providing PNT services to cislunar and deep-space missions.

1 INTRODUCTION

In the next decade, mission activities will be burgeoning to establish a lunar basecamp as a waystation to other interplanetary missions in the Solar system. NASA's Artemis program is a prime example of such endeavors. Other national entities, such as China, are also embarking on similar missions. Therefore, a reduction in the reliance on Earth for operating cislunar and deep-space missions is warranted. Today, cislunar missions heavily rely on the deep space network (DSN). However, DSN is a limited resource regarding availability, scheduling, and physical constraints to service cislunar and deep-space missions. DSN limited access reduces the mission and science throughput for cislunar and correlated deep-space missions. There is no position, navigation, and timing (PNT) system covering the cislunar space as there are global navigation satellite systems (GNSS) and other ground-based observation networks for Earth-based missions. At the same time, there is a limited body of knowledge discussing the realization and feasibility of an analogous Earth-independent PNT system for the vast distances of the cislunar space. A navigation system that can work independently of Earth's resources, such as the DSN, would enable more sustainable achievement of the cislunar and deep-space mission and scientific goals. An Earth and GPS independent navigation system can increase autonomous mission operations to a greater degree and improve the science/mission throughput. We address the lack of autonomy for cislunar and deep-space missions with the concept of a constellation of small spacecraft tactically placed in the cislunar region to observe objects in large portions of the cislunar space with minimal reliance on Earth's resources. In this paper, we present our studies' results into the baseline three-body (Circular Restricted Three-Body Orbits, CR3BP) orbits and the constellation configurations to achieve specific target goals for regional coverage.

The CAPSTONE mission by the Advanced-Space corporation in collaboration with NASA will demonstrate state-of-the-art capabilities for autonomous navigation in cislunar space.[1] The mission

*Ph.D. Student, Department of Aerospace Engineering, Auburn University, Auburn, AL 36849
†Assistant Professor, Department of Aerospace Engineering, Auburn University, 211 Davis Hall, Auburn University, Auburn, AL 36849.
‡Chief Executive Officer, Kayhan Space Corporation, Boulder, CO 80301

will test and establish a flight technology readiness level (TRL) for the CAPS (Cislunar Autonomous Positioning System) autonomous navigation algorithm in NASA's Artemis Gateway near-rectilinear halo orbit (NRHO). There is no existing space-based PNT system for the cislunar region analogous to GNSS services for the near-Earth environment. However, some works are available in the literature that we can leverage to develop our concept. A primer on cislunar space is provided by Holzinger et al.[2] The primer posits that optical telescopes are a suitable observation platform compared to other solutions because of the PNT payload power requirements. TrustedSpace technologists Bolden et al.[3] conducted a trade study on 13 different constellation configurations (i.e., combinations of LEO, GEO, 3:1 resonant, Lagrange-Point, and Lissajous orbit-based observers). The trade study compared the satellite system's ability to observe and cover the cislunar region for space situational awareness (SSA) purposes. The best design achieved a maximum coverage of around 27 percent of the region. Purdue University's Gupta et al.[4] identified a family of circular restricted three-body problem (CR3BP) orbits (i.e., 2:1 resonant) that span the GEO region at their perigee and the Moon at the apogee. In our concept, we also have identified one such 2:1 resonant orbit with these characteristics and employ it in our baseline orbit configurations. Vendl and Holzinger[5] established an observability accessibility metric for assessing a given CR3BP orbit's capability to observe a part of the cislunar region under Sun illumination conditions. Based on this metric, they identified that CR3BP orbits whose orbital period is in 1:1 resonance with the synodic period of the Earth-Moon CR3BP system are the best vantage points for observation coverage. In our concept, we plan to utilize space-borne optical telescopes and inter-spacecraft communication links to minimize the reliance on Earth for PNT services. Hill et al.[6] demonstrated that it is possible to perform tracking of objects in the lunar vicinity with satellite-to-satellite tracking (SST) with their introduction of the LiAISON navigation algorithm. However, they also state that the shorter the period of the observed orbits, the better it is in terms of accuracy and that not all orbits are conducive to LiAISON. Thompson et al.[7] conducted a more recent investigation into cislunar orbit determination and tracking using simulated optical measurements. They identified that, for any meaningful accuracy for tracking, observations covering at least half of the orbital period of the target orbit are needed.

By analyzing orbit configurations and satellite placement we establish a baseline configuration for a concept cislunar PNT system. We believe this knowledge will serve the space community in identifying the requirements and limitations of cislunar autonomous navigation systems that work with minimal reliance on the Earth-based resources. We introduce the cislunar PNT constellation concept and evaluation metrics for the feasibility studies in section 2. In section 3, we describe assumptions and methods for the analysis of a PNT constellation concept. In section 4, we present the results and discussion for different constellation configurations.

2 THE PNT CONSTELLATION CONCEPT

In our PNT constellation concept, we deploy a predefined number of spacecraft across a set of candidate orbits. We initially limit the analysis to candidate orbits in the cislunar plane. From here on out we refer to these spacecraft as the observers. We assume these observers are equipped with technology and payload for inter-satellite links (ISLs) with other transiting spacecraft in or near the cislunar planar region. Using the ISL technology, the observers communicate amongst themselves to transfer measurements and observations. Communication between two observers is only possible when the distance between the two satellites is less than an hypothetical ISL range. Any observer can also provide precise time and state information to any transiting spacecraft (i.e., one that is

not part of the PNT constellation), assuming that the transiting spacecraft is equipped with an ISL receiver. The ability to communicate with transiting spacecraft effectively establishes a PNT service that relies minimally on the Earth-based communication resources. Figure 1 is illustrating our PNT constellation concept.

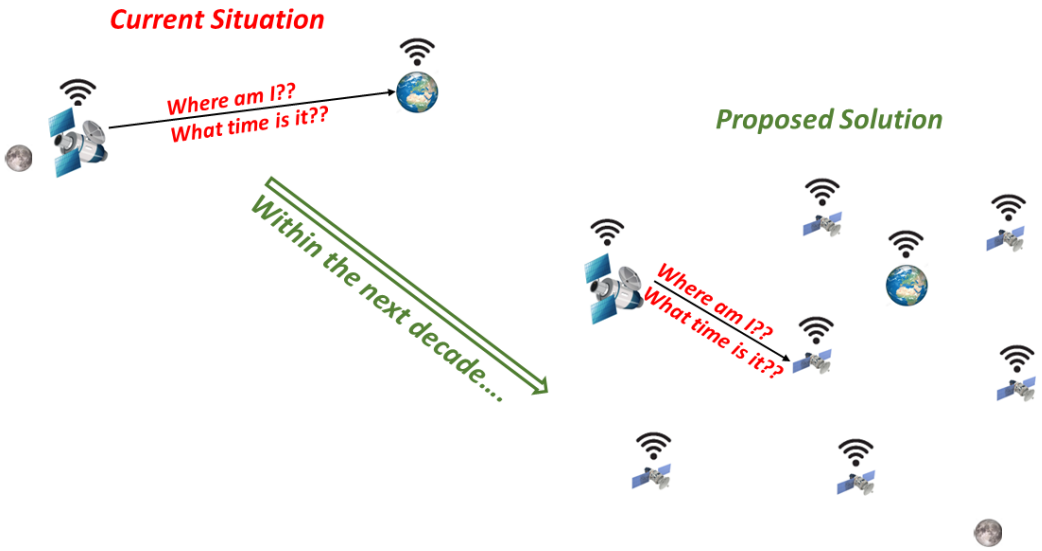

Figure 1: Proposed PNT Constellation Concept

2.1 Distributed Orbit Determination

To analyze a PNT constellation concept, a future distributed orbit determination (OD) algorithm is postulated. In this distributed OD concept, each of the observers collects measurements of other observers and targets in the cislunar region over time and periodically performs orbit determination independently of Earth and other observers. We assume the distributed OD system can support multiple measurement models and measurement data formats for the target objects. This distributed OD algorithm is able to provide precise time and state estimates for all the observers and also any transiting target spacecraft in the cislunar region, relying minimally on Earth's communication/observation resources. All the goals set forth and analyses conducted in the work presented in this paper are in service of this distributed orbit determination algorithm. For example, we postulate that this distributed OD algorithm will provide good estimates if there are measurements collected at least once per week. We translate this minimum frequency of measurements into target coverage metrics from the candidate constellation designs.

2.2 The PNT Constellation Figures-of-Merit Definitions

To help guide the feasibility studies, we introduce specific metrics to judge the quality of a PNT cislunar constellation. This section presents the metrics used to assess the various mission design choices for the PNT constellation concept.

2.2.1 Communication Opportunity A communication opportunity occurs when an observer is within the communication distance range (dictated by the ISL payload distance range) of other observers or other targets transiting the cislunar region. There may or may not be any line-of-sight and visibility requirements for communications. In this work we assume both of the requirements.

2.2.2 Observation Opportunity An observation opportunity occurs when an observer is within the observation distance range (dictated by the observation payload distance range) to observe other observers, locations in space or other targets transiting the cislunar region. Although the optical telescopes considered for our PNT constellation concept typically have observation ranges defined in terms of angles, we are choosing to use the observation distance to identify an observation opportunity to first remain agnostic to telescope specifications. In this work we assume line-of-sight and visibility requirements for observation opportunities. To simplify analysis in our preliminary studies, we assume that if a target is observable, it is also possible to communicate with it.

2.2.3 Coverage Target A coverage target is any one of observers, a transiting spacecraft, an unknown object, or simply the location under observation.

2.2.4 Coverage It is defined as the communication/observation opportunity between any observer and a coverage target.

2.2.5 Coverage Density Coverage density is a metric that provides a measure of the probability of coverage for a given coverage target over a given time window. In the current work, the coverage density is a ratio of total timesteps for which there is a communication/observation opportunity and the total simulation timesteps.

2.2.6 Coverage Interval Coverage interval is a metric used to define the existence of continuous opportunities for communications/observations between an observer and a coverage target. Coverage interval is the time interval for which any target located at the given position is in the vicinity of one or more other spacecraft within a given distance range for ISL communications/observations. The interval can be a unit of time or the number of timesteps in the simulation. In this work we use the number of timesteps to measure coverage interval.

2.2.7 Number of Coverage Intervals The number of coverage intervals is a metric that specifies how many continuous coverage opportunities are available within a given simulation time window between an observer and a coverage target.

2.2.8 Average Coverage Interval This metric is defined as the average of all of the coverage intervals within a given time window. This metric is computed in terms of timesteps within a given time window.

2.2.9 Temporal Graph A graph is a collection of nodes and edges that collectively capture the binary relationships among nodes.[8] A temporal graph[9] is a special version of the regular graph where the nodes have a timestamp associated with them. This facilitates the identification of binary relationships over time. The regular graphs are static in terms of time and cannot capture how the relationships evolve over time.

2.2.10 All-Pairs-Shortest-Paths As stated in Section 2.1, coverage opportunity frequency of once a week is considered good coverage. To capture the frequency of coverage for each given constellation configuration over time, we build a temporal graph of all coverage opportunities possible within the given simulation time window for each constellation configuration. We then use the all-pairs-shortest-paths[8] measure in the temporal graph to assess the evolution of coverage over time. Since the nodes in the temporal graph are indexed with a timestamp, there are as many possible

nodes for a given observer as there as simulation timesteps. However, only a few of these nodes are expected to have edges with other observer nodes over time. Our goal with this metric is to identify how dense and frequent the coverage opportunities are.

3 FEASIBILITY STUDY DEFINITION

This section presents the goals, assumptions and methods to design orbit and constellation configurations for a concept PNT system.

3.1 Scope

The analyses presented in this paper are limited to a planar region nearby the Earth-Moon plane. Since this work is a preliminary study into the coverage characteristics provided by the cislunar PNT constellation concept, we first consider a relatively smaller and tractable problem with planar regional focus.

3.2 Goals

Different mission requirements may drive the design of a cislunar PNT constellation. For this particular work, the set of goals that defines the scope of our feasibility studies is as follows:

3.2.1 Cislunar Regional Coverage The first requirement for a cislunar PNT constellation establishes the coverage density for the cislunar region. We target a number of coverage intervals of once a week within the given simulation time window per observer per coverage target. The area considered for this requirement is the area of an observation plane in the Moon's orbital plane. This observation plane has concentric circles with radius starting from 32145 km to 1.2 times the characteristic length (389703 km) of the Earth-Moon system.

3.2.2 Flow-of-Information Quality Since the PNT service is provided by the observers distributed in the chosen constellation configuration, this requirement establishes that information must flow within a given constellation design. We believe there should be a path of information flow for all pairs of observer spacecraft in the constellation over time. To construct a measure of how well information flow through the constellation over time, we model the constellation configuration time evolution (i.e., the spacecraft location at each epoch) as a temporal graph. On this temporal graph we compute all-pairs-shortest-paths[9] out of all possible communication-linking opportunities among the observer spacecraft in the constellation for a given time window. Higher the number of all-pairs-shortest-paths, higher the confidence that information flows well through the constellation configuration.

With these two goals, we assess the quality of the orbit and constellation configurations chosen in terms of coverage density, frequency of coverage intervals over time.

3.3 Constellation Design and Analysis Procedures and Methods

In this work, feasibility studies are conducted in three steps for each constellation design. First, we chose a constellation orbit configuration in the Earth-Moon CR3BP model. Next, we propagate the CR3BP orbits within N-body gravitational dynamics using ephemeris data. The N-body equations of motion are formulated in the Earth-centered J2000 frame. Second, we choose the number and phasing of the observers to be placed along the N-body orbits and compute coverage metrics as defined in Section 2.2. Third, we construct a temporal graph for the given simulation time window that captures the opportunities for communications among the observers in the chosen constellation

configurations. The all-pairs-shortest-path metric introduced in Section 2.2.10 serves as a measure of the connectivity density over time in the constellations. Following are the details of each step.

3.3.1 Orbit Configuration Design We primarily leveraged the JPL's three body orbits catalog located on JPL's Solar System Dynamics website[10] for selecting the candidate orbits for planar coverage. The website provides plots of the orbits in the catalog. We visually inspected all available orbit families in this catalog to arrive at a candidate configuration. The approach we took to select candidate orbits is to select multiple orbits from various families that can span a good portion of the CR3BP Earth-Moon plane. We specifically chose orbits that have instantaneous apses close to points of interest (i.e., Earth, Moon and Lagrange points), providing a means to transfer information to and from the Earth. We also attempted to select the orbits with foreseeable low station-keeping costs. In lack of actual information, we employed the stability index of each of the orbits included in the baseline configuration as a proxy for the station-keeping cost. We assume lower the stability index, lower the station-keeping cost. This assumption warrant future verification within higher-fidelity station-keeping simulation.

3.3.2 Spacecraft Placement and Constellation Design After determining the orbit configuration, we choose the number of spacecraft per orbit together with the phasing of these spacecraft in their respective orbits. The spacecraft are assumed to be small spacecraft with a range of 25000 km for observations and communications. With these limitations, 1 - 6 spacecraft per orbit are selected. We examined three types of spacecraft placement strategies along each orbit, considering 1) equidistant placement in time of flight, 2) equidistant placement in orbit arc-length, and, 3) random-distant placement in time of flight. However, in our preliminary analyses, we found the third option (random-distant placement in time of flight) to be the best strategy. For computing the coverage provided by a given constellation configuration, we divided the cislunar planar region under consideration in the Earth-centric J2000 frame into concentric circles spaced 1000 kilometers apart. Each such circle is then divided into points along the circle of equal arc-length. The arc-length is chosen to be same across all the circles, hence, the bigger the circle, the higher the number of points along the circle (A snippet of the concentric circular region is shown in Figure 2). Then, the coverage for the entire region is computed as the coverage from the spacecraft distributed in the constellation configuration for each of the points along the circles.

Prior to computing the coverage metrics, the CR3BP orbits selected from the orbit configuration analysis are transformed and corrected[11] into Earth-centric J2000 frame orbits under the N-body effects in ephemerides provided by the NASA SPICE tool.[12]

To compute the coverage metrics for each of the points chosen in the concentric circular cislunar plane, we compute the range vector, $\vec{V}$, from the observer to the target points in the cislunar plane and enforce a maximum range for the magnitude of this range vector. We also enforce exclusion cones for the range vector as shown in Figure 3, to compute the coverage metrics. In lieu of an actual target spacecraft to track, we substitute a target point on the cislunar concentric circular plane.

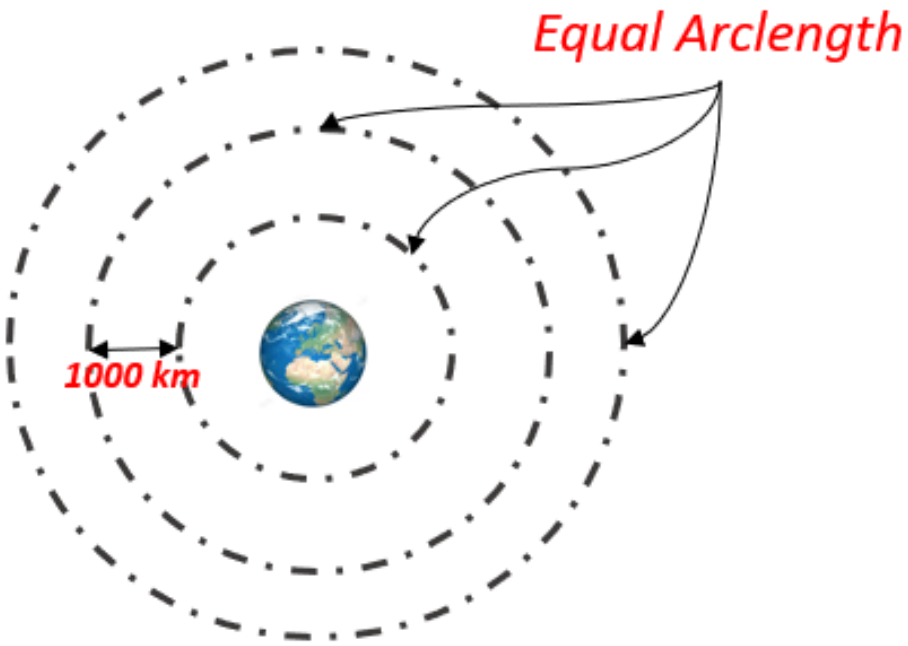

Figure 2: Selected Points for Cislunar Coverage Computations (Earth-centric J2000-Frame)

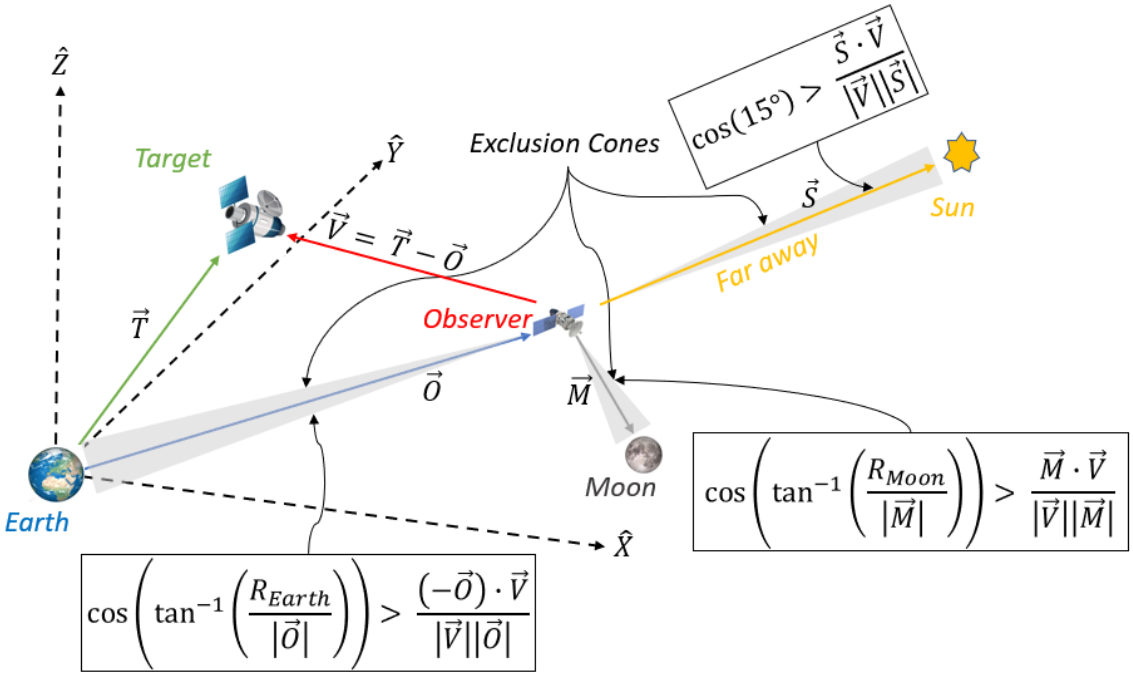

Figure 3: Eclipse Exclusion Cones for Coverage (Earth-centric J2000 Frame)

3.3.3 Flow of Information Analysis In this analysis, we derive a temporal graph (i.e., a graph which varies with time[9]) from the connectivity opportunities among all of the constellation observers within a given time window for a given communication range. In this graph we create nodes such that each observer pair within the given distance range generates two nodes. Importantly, a timestamp index is attached to the node name upon node creation (an example is provided in Figure 4). We then employ the all-pairs-shortest-paths algorithm called the Floyd-Warshall algorithm[8] to derive paths for each pair of observers indexed by timestamps. The all-pairs-shortest-paths metric for this temporal graph provides a measure of the density of connections available for a given constellation configuration and a given connection distance range over time. If there are N nodes in the temporal graph, there are $(N * (N + 1)/2 - N)$ possible all-pairs-shortest-paths. The density of connections is a percentage of all possible all-pairs-shortest-paths in the temporal graph. The higher this percentage the better the flow of information is over time.

Timestamped Communications

Timestamp	Source	Target
0	A	B
1	A	C
1	A	E
3	E	D
5	B	C
9	B	D
14	D	B
20	A	D

Temporal Graph

(Undirected)

Source	Target	Weight
A0	B0	E-8
A0	A1	1
A1	C1	E-8
A1	E1	E-8
E1	E3	2
E3	D3	E-8
B0	B5	5
C1	C5	4
B5	C5	E-8
B5	B9	4
D3	D9	6
B9	D9	E-8
D9	D14	5
E9	E14	5
D14	B14	E-8
A1	A20	19
D14	D20	6
A20	D20	E-8

Figure 4: Temporal Graph Example

4 RESULTS AND DISCUSSION

This section presents results for two reference orbit configurations and three constellation configurations (derived using the two orbit configurations) following the steps described in Section 3.

4.1 Orbit Configurations

There are two orbit configurations derived from the orbit configuration analysis. Figures 5 and 6 are showing the smaller and larger planar orbit configurations chosen using the method described

in Section 3.3. The smaller configuration comprises of one 2:1 resonant orbit (Red), eleven 3:1 resonant orbits (Green), seven 3:2 resonant orbits (Magenta), six L_1 and L_2 Lyapunov orbits (Brown). The larger configuration comprises, in addition to the smaller configuration orbits, additional six L_1 and L_2 orbits and eighteen 3:4 resonant (Purple) orbits. Together, these orbits are covering a vast region of the planar cislunar region. The properties of the CR3BP orbits from the smaller and larger configurations are shown in Table 1.

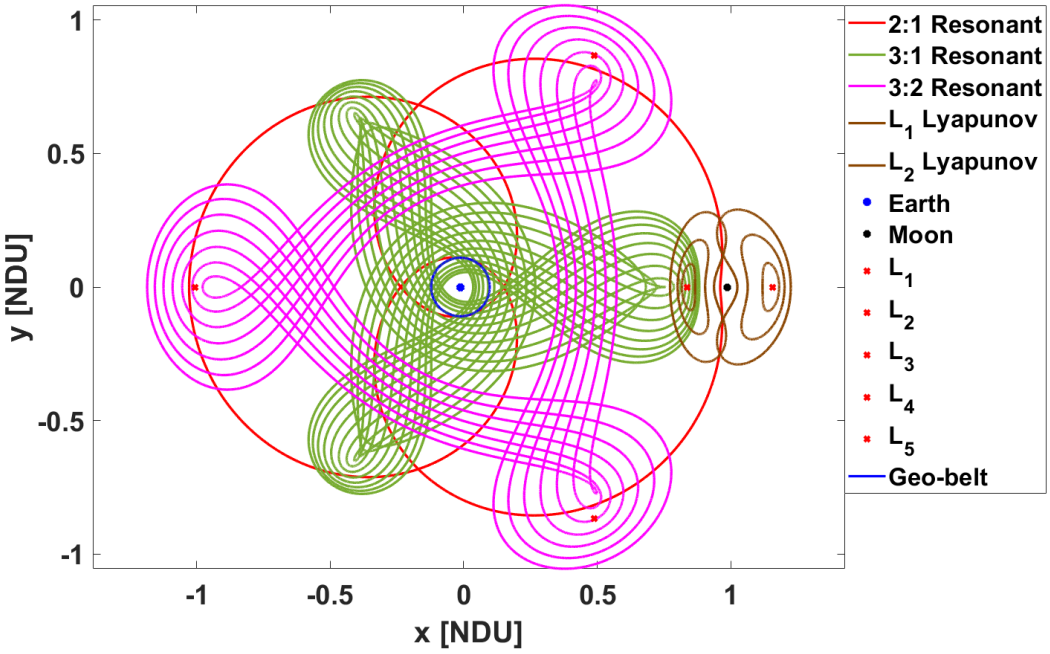

Figure 5: Smaller Orbit Configuration for Planar Coverage (CR3BP Rotating-Frame)

Table 1: CR3BP Orbit Properties

Orbit-Type	Orbital-Period-Range [Days]	Jacobi-Constant-Range	Stability-Index-Range
Resonant 2:1	26.46528	1.2895	-
Resonant 3:1	27.9155 - 28.8839	2.7536 - 3.3359	7.1064 - 1.6565
Resonant 3:2	55.9346 - 53.9632	2.7924 - 3.0042	1.0956 - 1.0000
Resonant 3:4	100.227 - 111.7998	2.923 - 2.1492	168.6084 - 2.0226
Lyapunov L_1	18.6718 - 12.0963	3.0063 - 3.1781	158.8475 - 1220.9000
Lyapunov L_2	19.7619 - 14.9721	3.0047 - 3.1698	113.2377 - 712.0446

4.2 Constellation Designs and Coverage Metrics

An important requirement for providing ample coverage of the cislunar region is having a good number of observer spacecraft in this region. What qualifies for a good number is not a trivial question to answer. We experimented with three constellation configurations that we label small, medium and large configurations as shown in Table 2. Table 2 is showing three configurations with number of orbits chosen from each orbit type and the number of observers per each of those

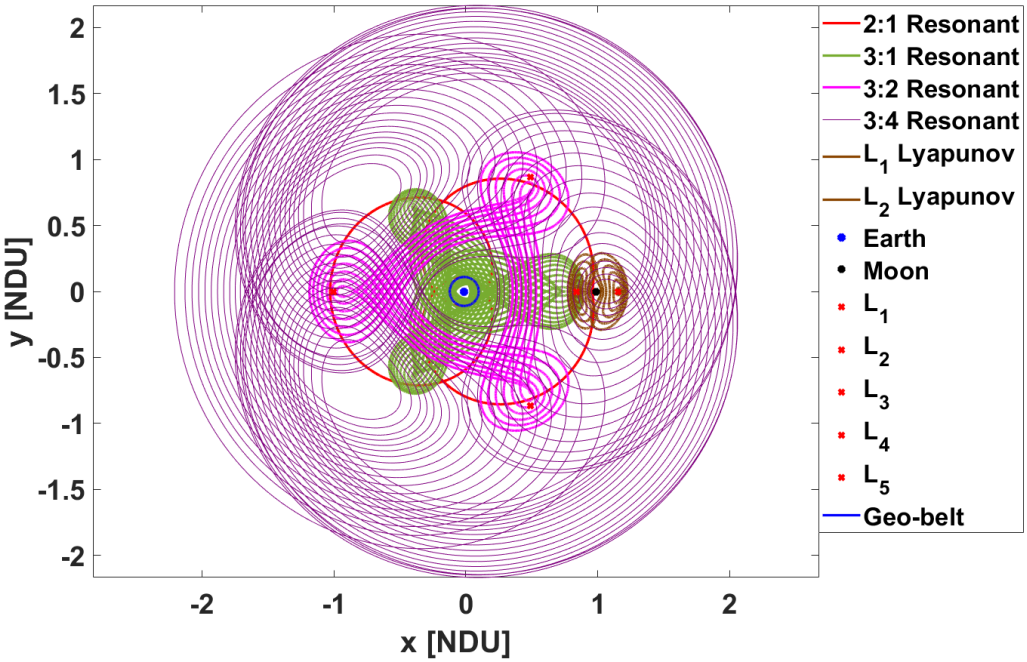

Figure 6: Larger Orbit Configuration for Planar Coverage (CR3BP Rotating-Frame)

orbits. The last row in the table is showing the total number of observers in each configuration. The observers in each of the constellation are randomly phased in their orbits. The CR3BP orbits are then transitioned into an ephemeris-based higher-fidelity dynamical model using a multiple-shooting algorithm. In the higher-fidelity model, the orbital motion is propagated in the Earth-centric J2000 coordinate frame under the ephemeris N-body attraction of the Earth, Moon, Sun, and Jupiter. The initial epoch chosen for the ephemeris propagation is January 1st, 2023 midnight in barycentric time (TDB). The orbits are corrected for a duration of ninty days with a timestep of twenty minutes. We chose a twenty minute timestep after computing the maximum inertial speed (6.31 kilometers per second) in the ephemeris orbits and calculating that to traverse 25000 kilometer range (i.e., the assumed ISL range) at this maximum speed takes at least an hour. Figure 7 is showing the collection of the 30 observer orbits in the smaller constellation as plotted in the Earth-centric J2000 coordinate frame. Figure 7 is showing the Moon's orbit and the ephemeris orbits inclined to the fundamental plane (Earth's Equator) of the Earth-centric J2000 frame at approximately 27.68 degrees. In this reference frame the Ecliptic (The plane Earth's motion around the Sun) is inclined to the Earth's Equator by about 23.4 degrees. The 25000 kilometer range of the observers allows for coverage of the targets in the Eclipic plane as well.

Table 2: Constellation Configurations

Orbit-Type	Small	Medium	Large
Resonant 2:1	1, 6/1	1, 6/1	1, 6/1
Resonant 3:1	11, 1/1	11, 3/1	11, 3/1
Resonant 3:2	7, 1/1	7, 3/1	7, 3/1
Resonant 3:4	NA	NA	18, 1/1
Lyapunov L_1	3, 1/1	3, 1/1	6, 1/1
Lyapunov L_2	3, 1/1	3, 1/1	6, 1/1
Total	30	66	90

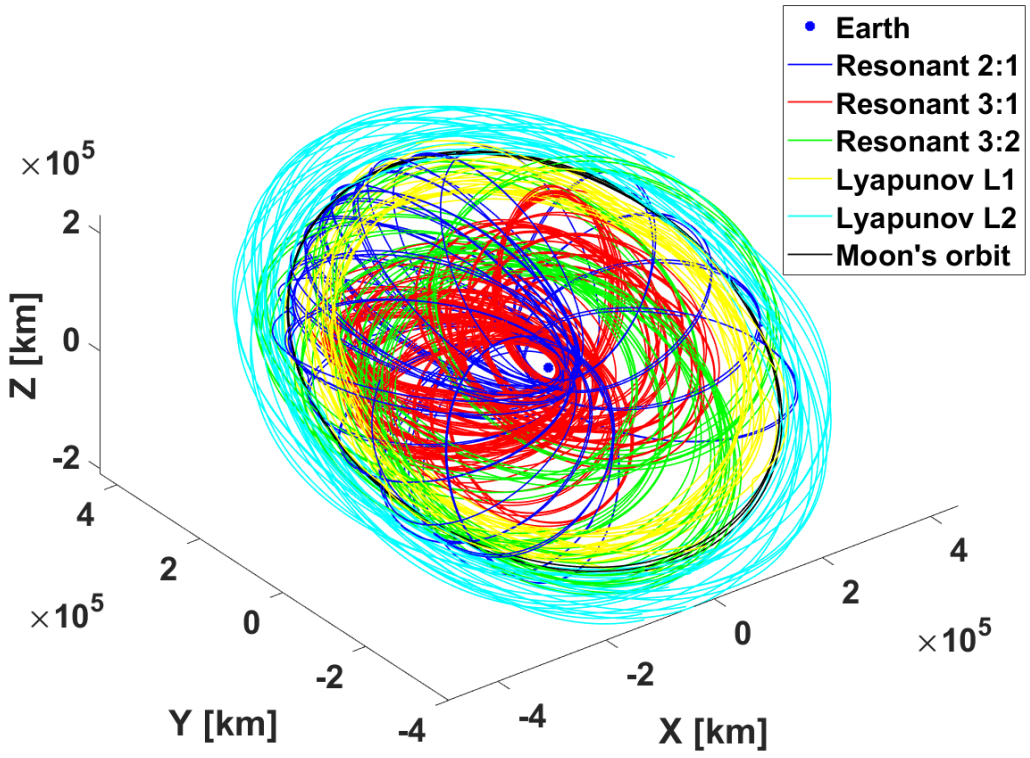

Figure 7: Smaller Constellation Orbits (Earth-centric J2000-Frame)

To compute the coverage metrics for the three constellation configurations, we first construct an observation plane in the J2000 reference frame. This observation plane is inclined to the Earth's Equator by the average inclination of the Moon. To construct this observation plane, we first construct a plane comprised of concentric circles with equal arclength observation points on the Equator of the Earth (we get a total of 338650 observation points). We then apply the 3-1-3 coordinate transformation to the plane of Moon's motion around the Earth. To do so, we first rotate the Equatorial observation plane (actually, each of the observation points on this plane) by a right ascension of 0 degrees with respect to the J2000 Z-axis. We then rotate the resulting observation plane with respect to the J2000 X-axis by the average inclination of the Moon's orbital plane. Finally we rotate the

resulting observation plane with respect to Z-axis of Moon's orbital perifocal frame by an argument of perigee of 0 degrees. Figure 8 is showing the resulting observation plane used for the coverage metrics.

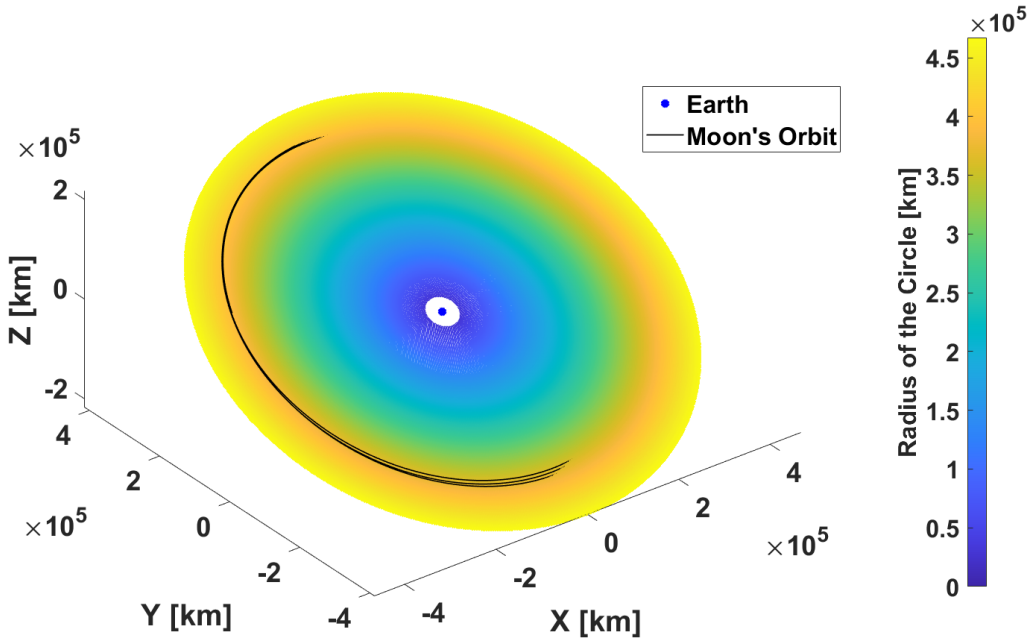

Figure 8: Observation Plane for Coverage Metrics (Earth-centric J2000-Frame)

To assess the three constellation configurations, we computed the coverage metrics defined in Section 2.2 for all the observation points chosen on the observation plane for each of the configurations using the method described in Section 3.3.2.

The small configuration results are presented in Figures 9, 10 and 11 respectively. Figure 9 is showing the coverage-density collected for 90 days at each of the observation points in the observation plane. Figure 10 is a histogram of number of coverage intervals. Figure 11 is a histogram of average coverage interval. We computed the number of observation points with at least 13 coverage intervals (there are about 13 weeks in the 90 day simulation window) to be 182155 out of a total of 338650, bringing the coverage percentage to 53.79. The average coverage interval for observations points with at least 13 coverage intervals is 10.91 timesteps or 3.6 hours.

The medium configuration results are presented in Figures 12, 13 and 14 respectively. Figure 12 is showing the coverage-density collected for 90 days at each of the observation points in the observation plane. Figure 13 is a histogram of number of coverage intervals. Figure 14 is a histogram of average coverage interval. We computed the number of observation points with at least 13 coverage intervals to be 206720 out of a total of 338650, bringing the coverage percentage to 61.04. The average coverage interval for observations points with at least 13 coverage intervals is 21.02 timesteps or 7 hours.

The large configuration results are presented in Figures 15, 16 and 17 respectively. Figure 15 is showing the coverage-density collected for 90 days at each of the observation points in the observation plane. Figure 16 is a histogram of number of coverage intervals. Figure 17 is a histogram of average coverage interval. We computed the number of observation points with at least 13 cov-

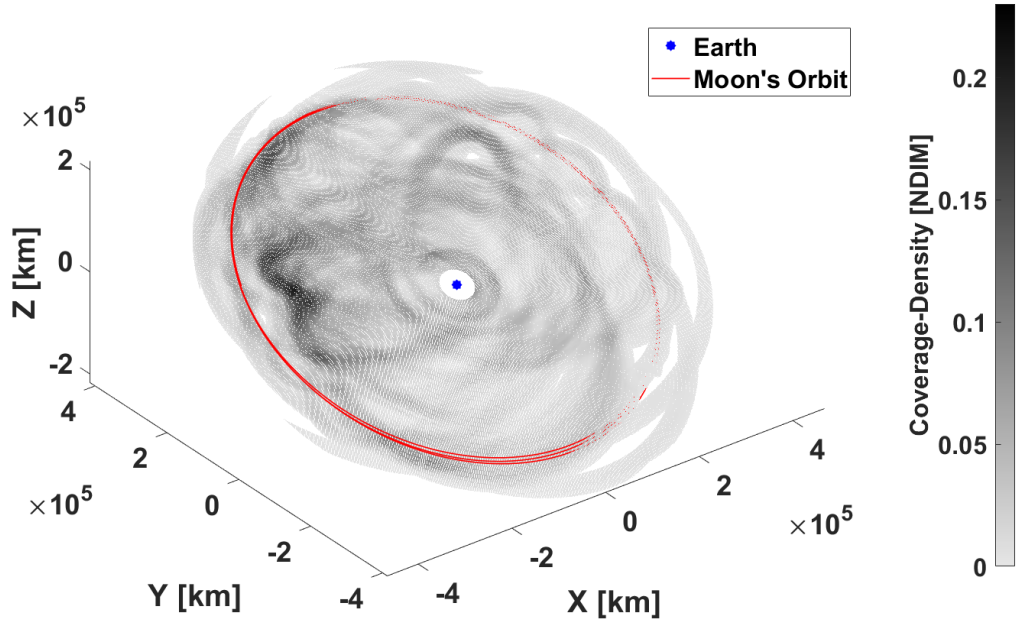

Figure 9: Coverage Density in the Observation Plane for Small Constellation (Earth-centric J2000-Frame)

erage intervals to be 271863 out of a total of 338650, bringing the coverage percentage to 80.28. The average coverage interval for observations points with at least 13 coverage intervals is 20.707 timesteps or 6.9 hours.

The coverage density shown in Figures 9, 12 and 15 is exhibiting an increasing trend. The smaller constellation is providing sparse coverage with a the exception of a few regions, yet when there is coverage (nearly 54 percent of the region has at least 13 coverage intervals) the average coverage interval (3.6 hours) is enabling of a the potential OD algorithm. An average coverage interval of 3.6 hours would reasonably allow collecting enough measurements to perform successful orbit determination with this constellation. The medium constellation has much better coverage density in the inner cislunar region than the smaller version, however, the percentage (61 percent) for coverage intervals of at least 13 is not a drastic improvement given that the number of observers is more than doubled. For the medium constellation, increase in the average coverage interval (7 hours) is very promising for collecting plenty of measurements for a successful orbit determination. The large constellation predictably shows the highest coverage density, number of coverage intervals over 13 and the average coverage interval in the observation plane. The confidence level for the collection of required measurements for a successful orbit determination algorithm is also quite high with this configuration.

4.3 Characterization of Flow of Information in the Constellations

Table 3 is showing the metrics for flow of information in each of the three constellation configurations. The first data row of the table is showing the number of possible timestep-indexed observer nodes based on possible communication opportunities (recall, we assume a maximum communication range of 25000 kilometers) in each of the constellations. Second row is showing all possible

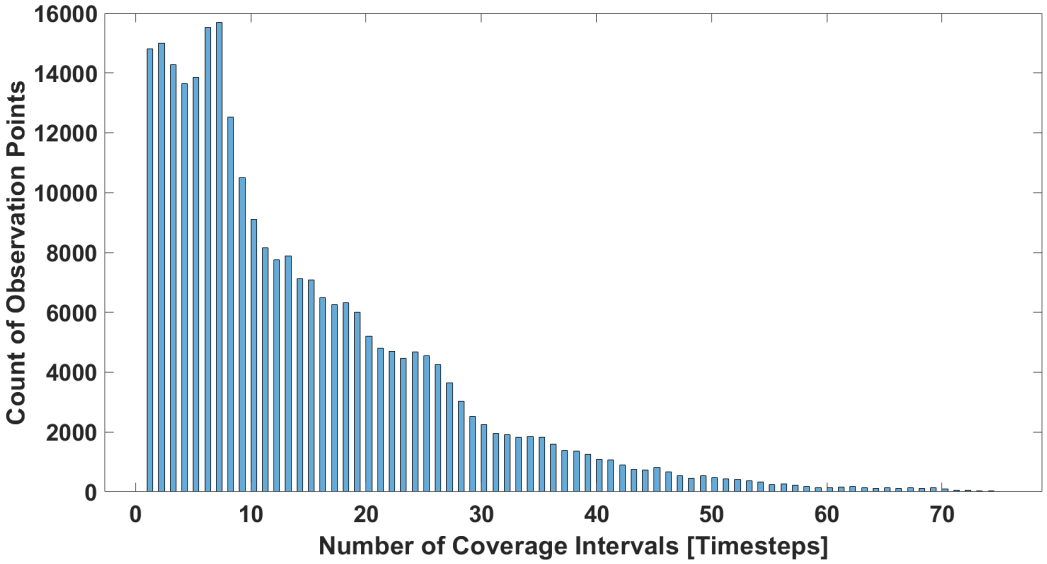

Figure 10: Number of Coverage Intervals Histogram for Small Constellation

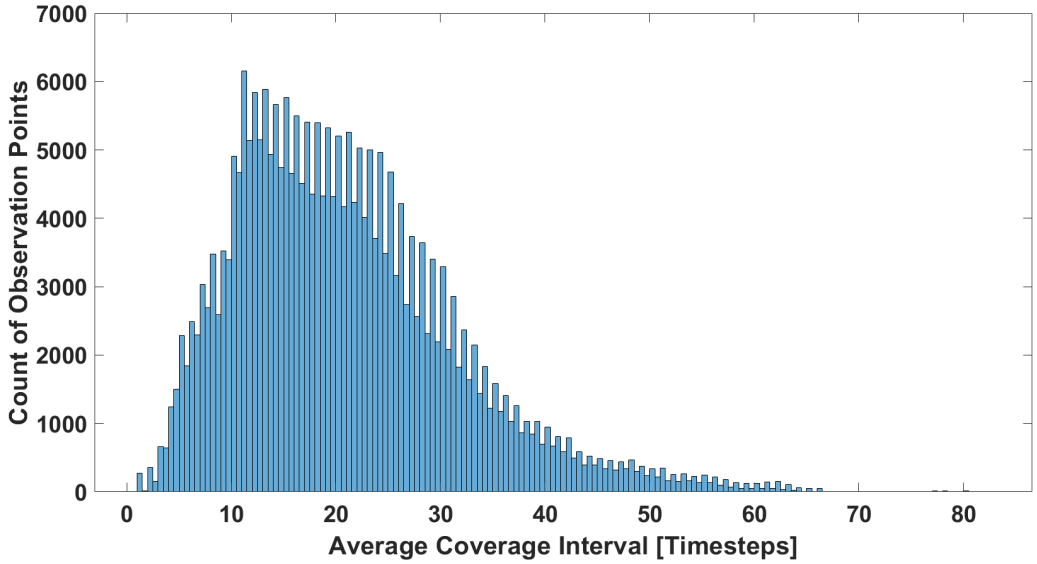

Figure 11: Average Coverage Interval Histogram for Small Constellation

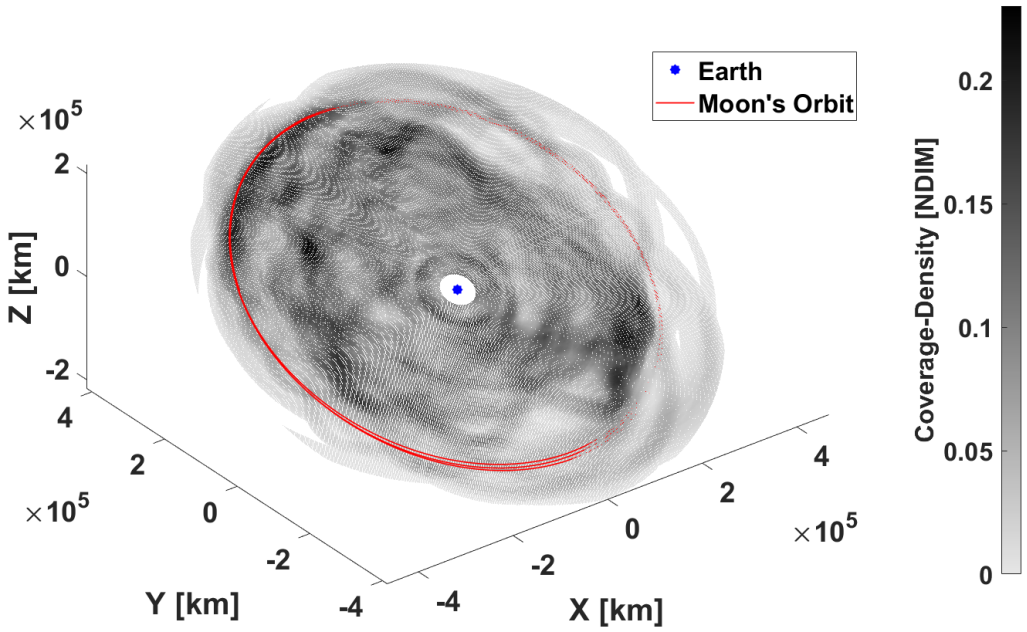

Figure 12: Coverage Density in the Observation Plane for Medium Constellation (Earth-centric J2000-Frame)

observer pairs per timestep. Third row is showing total timesteps (20-minute timestep) over the simulation time period (30 days). Fourth row is showing the number of all possible shortest paths (communication opportunities) among observer pairs for the entire simulation time period (computed using the fast Floyd-Warshall algorithm implementation in JuliaGraphs[13] package). Fifth row is showing the number of actual paths (communication opportunities) based on the orbital motion over the simulation time period. Sixth row is showing percentage of actual paths among the all possible paths. Seventh row is showing the average number of communication opportunities per observer per timestep. As can be seen in the seventh row, the small constellation has a very low number of connections indicating that this may not be suitable for the proposed PNT system. However, the medium and large constellations are looking promising for the PNT constellation.

Table 3: Flow-of-Information Metrics

Metric	Small	Medium	Large
Number of Nodes over Simulation Time	11373	40078	51891
Number of Node Pairs Per Timestep	435	2145	4005
Number of Timesteps for 30 Days	2161	2161	2161
Number of All Possible Paths	940035	4635345	8654805
Number of Actual Paths	12245	357849	732586
Percentage of Paths	1.3	7.72	8.46
Average Number of Connections Per Node	148	3094	4392

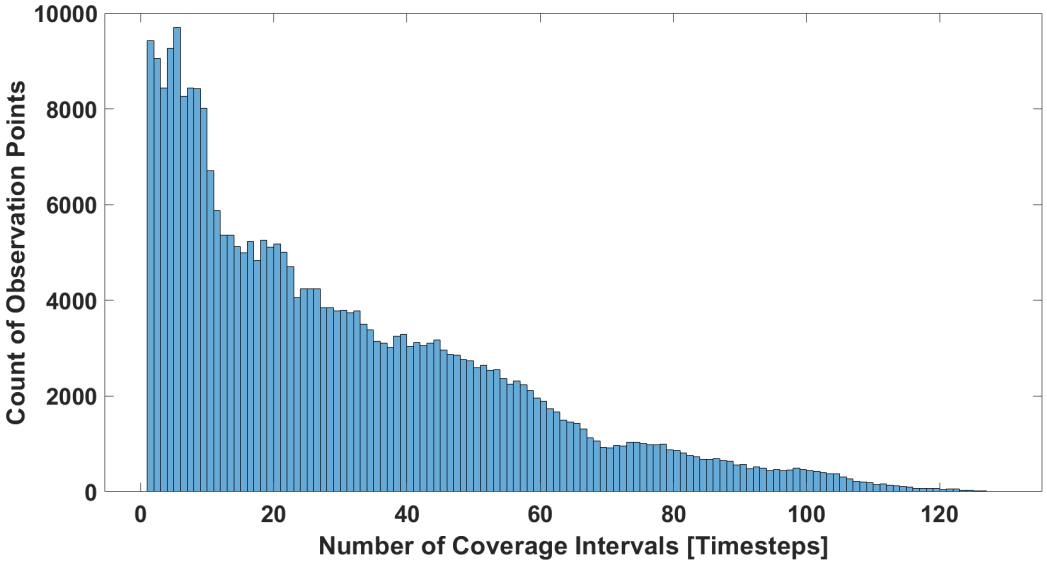

Figure 13: Number of Coverage Intervals Histogram for Medium Constellation

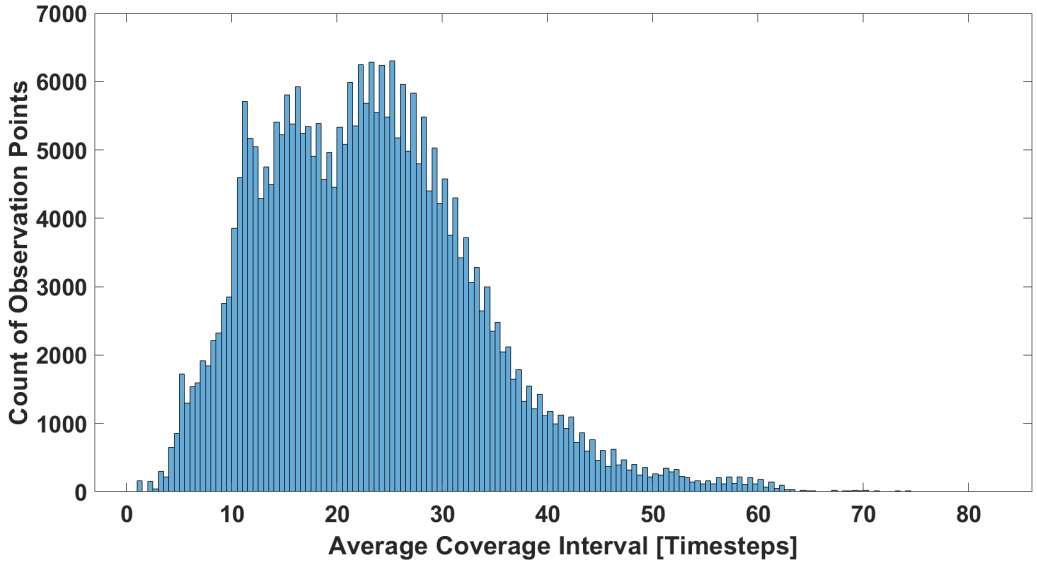

Figure 14: Average Coverage Interval Histogram for Medium Constellation

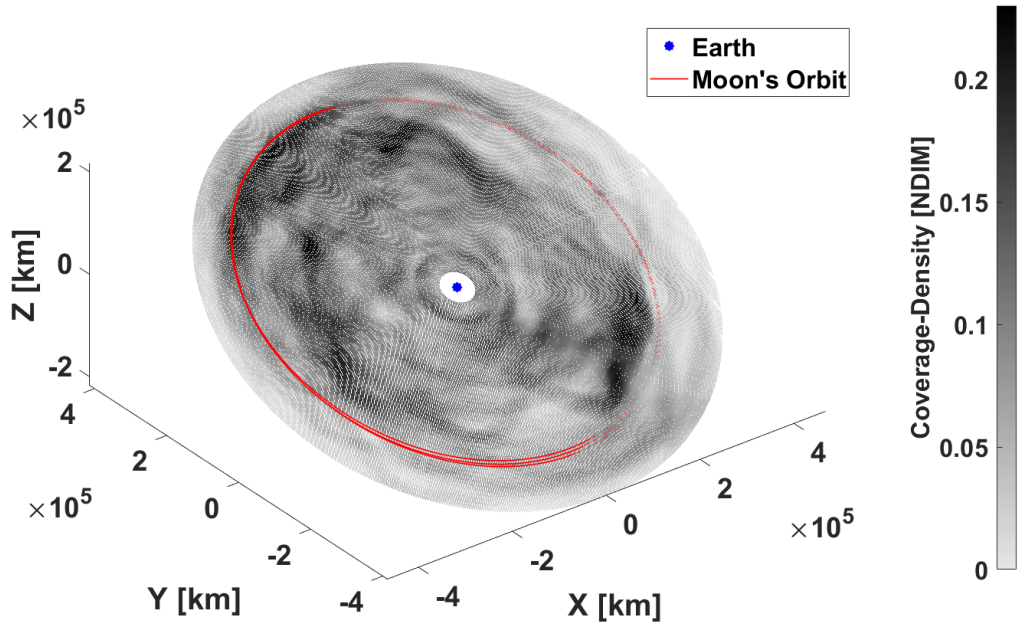

Figure 15: Coverage Density in the Observation Plane for Large Constellation (Earth-centric J2000-Frame)

5 CONCLUSION

We presented preliminary methods and results that aid determining the feasibility of a cislunar PNT constellation concept. We designed and examined two orbit configurations and three constellation configurations. We also defined metrics to judge the quality of each configuration. The metrics provide an assessment of how well the cislunar planar region is covered over time. Furthermore, the metrics are derived for orbital motion within ephemeris N-body dynamics. This higher fidelity orbital motion gives us confidence that the metrics computed are realistic and can sustain the PNT constellation concept well. Although, further analysis is required to establish sensitivity of the results to the modelling assumptions, including, but not limited to, the initial epoch and the spacecraft placement.

REFERENCES

[1] B. W. Cheetham, T. Garder, and A. Forsman, "Cislunar Autonomous Positioning System Technology Operations and Navigation Experiment (CAPSTONE)," Las Vegas, NV, AIAA ASCEND, Sept. 2021.

[2] M. J. Holzinger, C. Chow, and P. Garretson, "A Primer on Cislunar Space," *AFRL Space Vehicles Directorate*, Vol. 1271, 2021.

[3] M. Bolden, T. Craychee, and E. Griggs, "An Evaluation of Observing Constellation Orbit Stability, Low Signal-to-Noise, and the Too-Short-Arc Challenges in the Cislunar Domain," *AMOS-Tech*, Wailea-Makena, HI, AMOS, Sept. 2020.

[4] M. Gupta, K. C. Howell, and C. Frueh, "Earth-Moon Multi-Body Orbit to Facilitate Cislunar Surveillance Activities," *AIAA/AAS Astrodynamics Specialist Conference*, 2021.

[5] J. K. Vendl and M. J. Holzinger, "Cislunar Periodic Orbit Analysis for Persistent Space Object Detection Capability," *Journal of Spacecraft and Rockets*, 2021, pp. 1–12.

[6] K. Hill, G. Born, and M. W. Lo, "Linked, Autonomous, Interplanetary Satellite Orbit Navigation (LiAISON) in Lunar Halo Orbits," *AIAA/AAS Astrodynamics Specialist Conference*, Lake-Tahoe, CA, AAS, 2005.

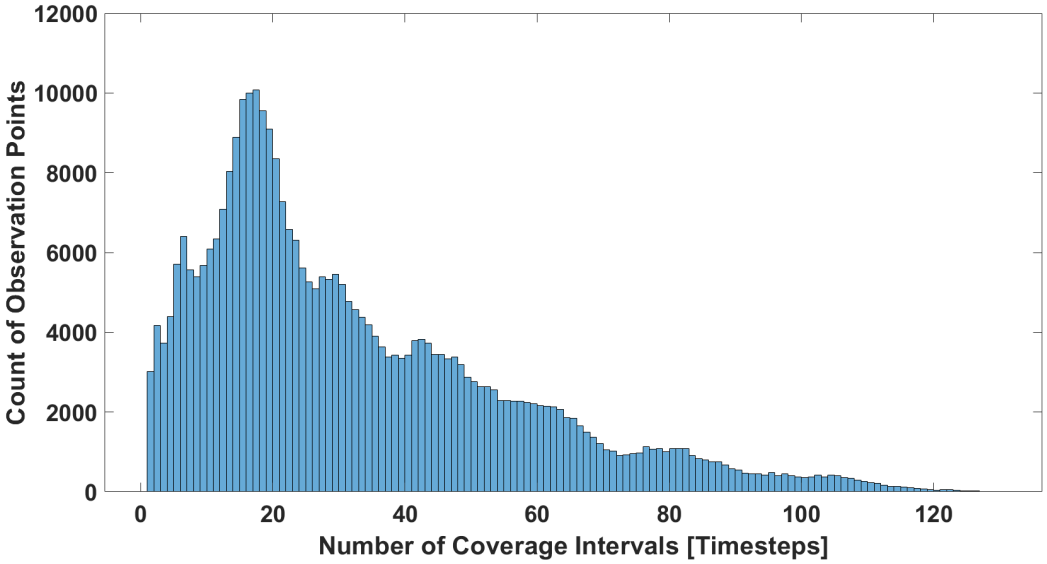

Figure 16: Number of Coverage Intervals Histogram for Large Constellation

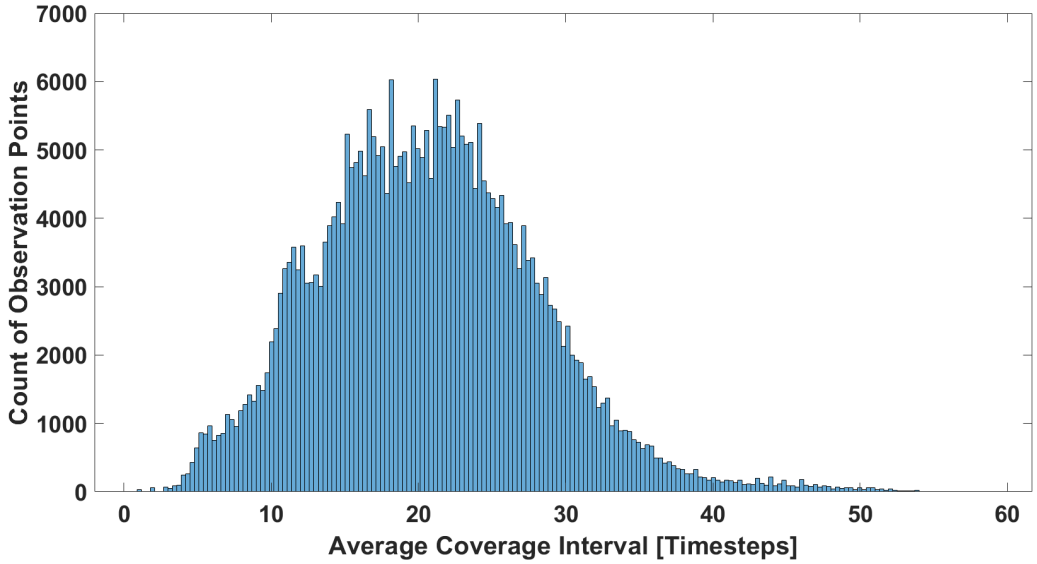

Figure 17: Average Coverage Interval Histogram for Large Constellation

[7] N. P. Re, M. R. Thompson, C. Meek, and B. W. Cheetham, "Cislunar Orbit Determination and Tracking via Simulated Space-Based Measurements," *AMOS-Tech*, Wailea-Makena, HI, AMOS, Sept. 2021.

[8] T. Cormen, C. Leiserson, R. Rivest, and C. Stein, *Introduction to Algorithms, third edition*. The MIT Press, MIT Press, 2009.

[9] V. Kostakos, "Temporal graphs," *Physica A: Statistical Mechanics and its Applications*, Vol. 388, No. 6, 2009, pp. 1007–1023, https://doi.org/10.1016/j.physa.2008.11.021.

[10] JPL, "Three Body Periodic Orbits Catalog," `https://ssd.jpl.nasa.gov/tools/periodic_orbits.html`. Accessed: 2022-03-03.

[11] L. R. Capdevila, "Transfer trajectories connecting the regions near the moon and triangular libration points in the earth-moon system with solar perturbations," *AIAA Scitech 2020 Forum*, 2020, p. 1464.

[12] C. H. Acton, "Ancillary data services of NASA's Navigation and Ancillary Information Facility," *Planetary and Space Science*, Vol. 44, No. 1, 1996, pp. 65–70. Planetary data system, https://doi.org/10.1016/0032-0633(95)00107-7.

[13] J. Fairbanks, M. Besançon, S. Simon, J. Hoffiman, N. Eubank, and S. Karpinski, "JuliaGraphs/Graphs.jl: an optimized graphs package for the Julia programming language," 2021.